Edith Cowan University

Research Online

Research outputs 2014 to 2021

3-2017

High-performance RF-sputtered Bi-substituted iron garnet thin films with almost in-plane magnetization

Mohammad Alam
Edith Cowan University

Mikhail Vasiliev
Edith Cowan University

Kamal Alameh
Edith Cowan University

Follow this and additional works at: https://ro.ecu.edu.au/ecuworkspost2013

 Part of the Engineering Science and Materials Commons

10.1364/OME.7.000676
Nur-E-Alam, M., Vasiliev, M., & Alameh, K. (2017). High-performance RF-sputtered Bi-substituted iron garnet thin films with almost in-plane magnetization. *Optical Materials Express*, *7*(3), 676-686.
https://doi.org/10.1364/OME.7.000676
This Journal Article is posted at Research Online.
https://ro.ecu.edu.au/ecuworkspost2013/2609

Research Article | Vol. 7, No. 3 | 1 Mar 2017 | OPTICAL MATERIALS EXPRESS 676

Optical Materials EXPRESS

High-performance RF-sputtered Bi-substituted iron garnet thin films with almost in-plane magnetization

M. NUR-E-ALAM,* MIKHAIL VASILIEV, AND KAMAL ALAMEH

Electron Science Research Institute, Edith Cowan University, 270 Joondalup Drive, Joondalup, WA 6027, Australia
**m.nur-e-alam@ecu.edu.au*

Abstract: Bismuth-substituted iron garnet thin films of high quality are prepared by using RF magnetron sputtering technique in pure argon (Ar) plasma. All the developed garnet films show high magneto-optic (MO) response after being optimally annealed across the visible range wavelengths. The garnet films display almost in-plane magnetization component with adequate Faraday rotation and relatively low optical absorption over a wide spectral range of frequencies from visible to the infrared. These garnet-type thin films demonstrate excellent MO properties together with very low coercive field of about 30 Oe, and can be used in a wide range of magneto optical applications, especially in magneto-plasmonic/magneto-photonic crystal based microdevices.

©2017 Optical Society of America

OCIS codes: (160.3820) Magneto-optical materials; (310.3840) Materials and process characterization; (130.3130) Integrated optics materials.

References and links

1. A. K. Zvezdin and V. A. Kotov, *Modern Magnetooptics and Magnetooptical Materials* (Institute of Physics Publishing, 1997).
2. G. B. Scott and D. E. Lacklison, "Magnetooptic properties and applications of Bismuth substituted iron garnets," IEEE Trans. Magn. **12**(4), 292–311 (1976).
3. S. Kahl, A. M. Grishin, S. I. Kharstev, K. Kawano, and J. S. Abell, "$Bi_3Fe_5O_{12}$ thin film visualizer," IEEE Trans. Magn. **37**(4), 2457–2459 (2001).
4. M. Nur-E-Alam, M. Vasiliev, and K. Alameh, "Nano-structured magnetic photonic crystals for magneto-optic polarization controllers at the communication-band wavelengths," Opt. Quantum Electron. **41**(9), 661–669 (2009).
5. H. Taketoshi, M. Yukio, and N. Junichiro, "Growth and characterization of Liquid-Phase Epitaxial Bi-Substituted iron garnet films for magneto-optic application," Jpn. J. Appl. Phys. **24**(10), 1316 (1985).
6. M. Huang and S. Zhang, "A new Bi-substituted rare-earth iron garnet for a wideband and temperature-stabilized optical isolator," J. Mater. Res. **15**(08), 1665–1668 (2000).
7. M. Zaezjev, M. C. Sekhar, M. Ferrera, L. Razzari, G. Ross, B. Holmes, M. Sorel, D. Hutchings, S. Roorda, and R. Morandotti, "Magneto-optic iron-garnet thin films for integrated optical applications," SPIE Newsroom (2007), doi:10.1117/2.1200701.0513.
8. E. V. Anoikin and P. J. Sides, "Plasma-activated chemical vapor deposition of Bismuth-substituted iron garnets for magneto-optical data storage," IEEE Trans. Magn. **31**(6), 3239–3341 (1995).
9. S. Kang, S. Yin, V. Adyam, Q. Li, and Y. Zhu, "$Bi_3Fe_4Ga_1O_{12}$ garnet properties and its application to ultrafast switching in the visible spectrum," IEEE Trans. Magn. **43**(9), 3656–3660 (2007).
10. T. Aichele, A. Lorenz, R. Hergt, and P. Gornert, "Garnet layers prepared by liquid phase epitaxy for microwave and magneto-optical applications – a review," Cryst. Res. Technol. **38**(78), 575–587 (2003).
11. M. Gomi, T. Tanida, and M. Abe, "RF sputtering of highly Bi-substituted garnet films on glass substrates for magneto-optic memory," J. Appl. Phys. **57**(8), 3888–3890 (1985).
12. D. Sylgacheva, N. Khokhlov, A. Kalish, S. Dagesyan, A. Prokopov, A. Shaposhnikov, V. Berzhansky, M. Nur-E-Alam, M. Vasiliev, K. Alameh, and V. Belotelov, "Transverse magnetic field impact on waveguide modes of photonic crystals," Opt. Lett. **41**(16), 3813–3816 (2016).
13. S. I. Khartsev and A. M. Grishin, "$[Bi_3Fe_5O_{12}/Gd_3Ga_5O_{12}]^m$ magneto-optical photonic crystals," Appl. Phys. Lett. **87**(12), 122504 (2005).
14. M. Nur-E-Alam, M. Vasiliev, and K. Alameh, "$Bi_3Fe_5O_{12}$: Dy_2O_3 composite thin film materials for magneto-photonics and magneto-plasmonics," Opt. Mater. Express **4**(9), 1866–1875 (2014).

#283035 https://doi.org/10.1364/OME.7.000676
Journal © 2017 Received 16 Dec 2016; revised 16 Jan 2017; accepted 19 Jan 2017; published 1 Feb 2017

Optical Materials EXPRESS

15. M. Vasiliev and M. Nur-E- Alam, V. A. Kotov, K. Alameh, V. I. Belotelov, V. I. Burkov, and A. K. Zvezdin, "RF magnetron sputtered $(BiDy)_3(FeGa)_5O_{12}$:Bi_2O_3 composite materials possessing record magneto-optic quality in the visible spectral region," Opt. Express **17**(22), 19519–19535 (2009).
16. M. M. Tehranchi, S. M. Hamidi, A. Hasanpour, M. Mozaffari, and J. Amighian, "The effect of target rotation rate on structural and morphological properties of thin garnet films fabricated by pulsed laser deposition," Opt. Laser Technol. **43**(3), 609–612 (2011).
17. A. Taabouche, A. Bouabellou, F. Kermiche, F. Hanini, S. Menakh, Y. Bouachiba, T. Kerdja, C. Benazzouz, M. Bouafia, and S. Amara, "Effect of Substrates on the Properties of ZnO Thin Films Grown by Pulsed Laser Deposition," Advances in Materials Physics and Chemistry. **3**(04), 209–213 (2013).
18. Q. Yang, H. Zhang, Q. Wen, and Y. Liu, "Effects of off-stoichiometry and density on the magnetic and magneto-optical properties of yttrium iron garnet films by magnetron sputtering method," J. Appl. Phys. **108**(7), 073901 (2010).
19. M. Nur-E-Alam, M. Vasiliev, K. Alameh, "Growth, characterisation, and properties of $Bi_{1.8}Lu_{1.2}Fe_{3.6}Al_{1.4}O_{12}$ garnet films prepared using two different substrate temperatures," Int. J. of Materials Engineering Innovation. **5**(3), 172–181 (2014).
20. M. Vasiliev and M. Nur-E-Alam, P. Perumal, Y. T. Lee, V. A. Kotov and Y. P. Lee, "Annealing behavior and crystal structure of RF-sputtered Bi-substituted dysprosium iron garnet films having excess cosputtered Bi-oxide content," J. Phys. D Appl. Phys. **44**, 075002 (2011).
21. M. B. Rabeh, R. Touatti, and M. Kanzari, "Substrate temperature effects on structural optical and electrical properties of vacuum evaporated Cu2ZnSnS4 thin films," Int. J. of Engineering Practical Research (IJEPR). **2**(2), 71 (2009).
22. A. H. Eschenfelder, *Magnetic Bubble Technology* (Springer-Verlag, 1980).
23. B. D. Cullity, *Elements of X-Ray Diffraction, 2nd edition* (Addison-Wesley Publishing Company, Inc., 1978).
24. Z. Abbas, R. M. Al-habashi, K. Khalid, and M. Maarof, "Garnet ferrite ($Y_3Fe_5O_{12}$) nanoparticles prepared via modified conventional mixing oxides (MCMO) method," European Journal of Scientific Research. **36**(2), 154–160 (2009).
25. S. Ruhela, and S. K. Srivastava, "Study of XRD Pattern of Mixed Composite of $MgTiO_3$ and ZnO," Int. J. of Innovative Research in Science, Engineering and Technology **2**(5), 1320–1322 (2013).

1. Introduction

Highly bismuth (Bi)-substituted MO garnet materials developed using RF magnetron sputtering are potentially very attractive for use in various technological applications such as magnetic memory, magnetoplasmonic devices, magneto-optic sensors, lightwave polarization controllers, and MO spatial or temporal light modulators [1–14]. Next-generation ultra-fast optoelectronic devices, such as light intensity switches and modulators for optical communications, high-sensitivity sensors for applications ranging from industrial and environmental or medical diagnostics, and high-speed flat panel displays for consumer electronics will likely benefit from using high-performance MO garnet materials [3,4,7,9]. MO garnet thin films possess strong Faraday or Kerr effects simultaneously with low optical losses in the visible and near infrared regions, and can be controlled with low applied magnetic fields. They are highly desirable for the development of low-power-consumption, small-footprint, cost effective and reliable photonic devices and sensors [2,5,9–12]. In advanced MO materials, controlling the hysteresis loop shape and magnetic anisotropy type is also of great practical importance, because this enables the magnetic materials to be switched with picosecond current pulses, thus making the power consumption low. It is of special interest to obtain new MO materials possessing low coercive field, so that the magnetization states can be switched using small current pulses. Special attention is devoted world-wide by researchers in the MO field to the selection of optimized material composition stoichiometry, achieving the synthesis of garnets with high Bi-substitution levels and improving the MO figure of merit [1–6,9–11,13–15]. Engineering the advanced materials possessing an optimized combination of the optical, magnetic, and MO properties is a challenging and quickly evolving research area of increasing importance today [15–21]. Note that the material inter-compatibility issues encountered in magnetic photonic and magnetic plasmonic crystals have previously been investigated and reported by our group [12,20], therefore, in this work, we focus the investigation on the properties of the newly-developed garnet material only.

Optical Materials EXPRESS

In this paper, we develop and investigate the performance of highly Bi-substituted garnet thin films, deposited using RF magnetron sputtering in conjunction with a sputtering target of stoichiometry $Bi_{2.1}Dy_{0.9}Fe_{3.9}Ga_{1.1}O_{12}$ and using an optimized high-temperature annealing process. Our main motivation for exploring this new garnet-film stoichiometry type was to research the optical and magnetic properties of a garnet material type, which is expected to possess somewhat "intermediate" magnetic anisotropy properties, i.e., having neither the in-plane nor perpendicular magnetization direction. Experimental processes for garnet layer fabrication and characterization are detailed in Section 2; the principal material property-related results achieved in high-performance MO thin film layers are discussed in Section 3. Finally, we draw a conclusion in Section 4.

2. Methods: synthesis and characterization of MO garnet layers

Several batches of highly-bismuth-substituted iron garnet thin films were sputtered from an oxide-base-mixed target of composition type $Bi_{2.1}Dy_{0.9}Fe_{3.9}Ga_{1.1}O_{12}$. Garnet layers were deposited on ultrasonically cleaned glass (Corning 1737, of refractive index 1.51 and negligibly small absorption coefficient) substrates using the optimized sputtering conditions and process parameters (summarized in Table 1) and different annealing processes were trialed to find the optimized annealing regime (in terms of both the temperature and time duration) for this garnet composition. The optimization of annealing regime was enabled by evaluating the best-obtained specific Faraday rotations at 532 nm and the film quality. Subsequently, thin film garnet layers on silicon (Si) substrates were also developed to investigate the surface morphology of these layers.

Table 1. Summary of the sputtering process parameters and conditions used to deposit the garnet thin film layers on glass substrates.

Process parameters /Composition type	Values & Comments
Sputtering garnet target stoichiometry type	$Bi_{2.1}Dy_{0.9}Fe_{3.9}Ga_{1.1}O_{12}$
Base pressure (Torr)	4-5 × 10^{-6}
Argon (Ar) pressure	≈2 mTorr
RF power / power density	150-220 W (3.3-4.4 W/cm^2)
Target to substrates distance	17-18 cm
Substrate stage temperature (°C)	Room Temperature (21-23 °C)
Substrate stage rotation rate (RPM)	35-37
Film thickness	250-1000 nm
Annealing temperature	530-670 °C
Annealing time duration	1-10 hours
Heating and cooling rates	5 °C/min
Annealing atmosphere	Air at normal ambient pressure

Multiple 10mm x 10mm and 20mm x 20mm batches (6-10 samples per batch) were prepared and annealed through different annealing regimes in order to identify the optimal regimes that result in large Faraday rotation without film surface damage. Only the reproducible results are shown in graphs related to Faraday rotation and MO quality. The substrate stage of the sputtering system was relatively small (about 4"), and the distance to target was relatively large (18cm), therefore within a 2" diameter within the center of substrate stage, only a slight thickness variation was seen (approximately 5%). In EDX experiments, insignificant stoichiometry variations were observed, and the results were averaged over several locations across the film surface.

Optical Materials EXPRESS

The physical thicknesses of the garnet layers were measured directly during the deposition using a quartz microbalance sensor, and indirectly after the deposition. The indirect thickness measurement method is based on measuring the transmission spectra of the deposited thin films, and spectrally fitting these transmission spectra with the modelled transmission spectra obtained using specialized thickness-fitting software [15]. The optical transmission spectra of both the as-deposited and post-annealed garnet films were measured using a UV/Visible spectrophotometer (Beckman Coulter DU 640B & Cary 5000), while the specific Faraday rotation of the annealed garnet layers were measured using a Thorlabs PAX polarimeter system in conjunction with a custom-made calibrated electromagnet. XRD measurements were performed by using a Siemens 5000D x-ray diffractometer. Energy dispersive spectroscopy (EDS) based elemental analysis was performed, using a Quantax Q100 system (Bruker.com), which confirmed the presence of all individual elements in the developed garnet thin films.

3. Results and discussion

In this work, garnet layers were crystallized using thermal processing boundaries of 580-670°C with a wide range of process durations (up to 10 hours). The process duration time was critical to obtaining the application specific material properties in a garnet layer as observed in present and previous annealing experiments carried out with garnet and garnet-oxide composite thin films [14,15,19,20]. Figure 1 shows the obtained x-ray diffraction data sets from two optimally annealed garnet samples (the optimized annealing regimes are indicated in the figure legend) and pattern indexing information. Theta-theta XRD measurements were performed using Cu $K\alpha_1$ collimated beam over a range of 2θ angles between 20° and 70°, at near-grazing x-ray radiation incidence. The measured XRD patterns revealed a good crystallinity and good growth conditions, as well as the presence of garnet phase formations of a highly Bi-substituted iron thin film layer on glass substrates. The angular positions of the x-ray diffraction peaks were determined using Jade 9 (MDI Corp.) software package (Peak-listing option). The x-ray diffraction peaks of the annealed samples align with the characteristic angles of the body-centered cubic lattice structure of garnets, confirming their nanocrystalline microstructure. The lattice constant for the synthesized garnet-type material were calculated using identifiable diffraction lines (Fig. 1) and the standard pattern indexing methods [22–24].

Optical Materials EXPRESS

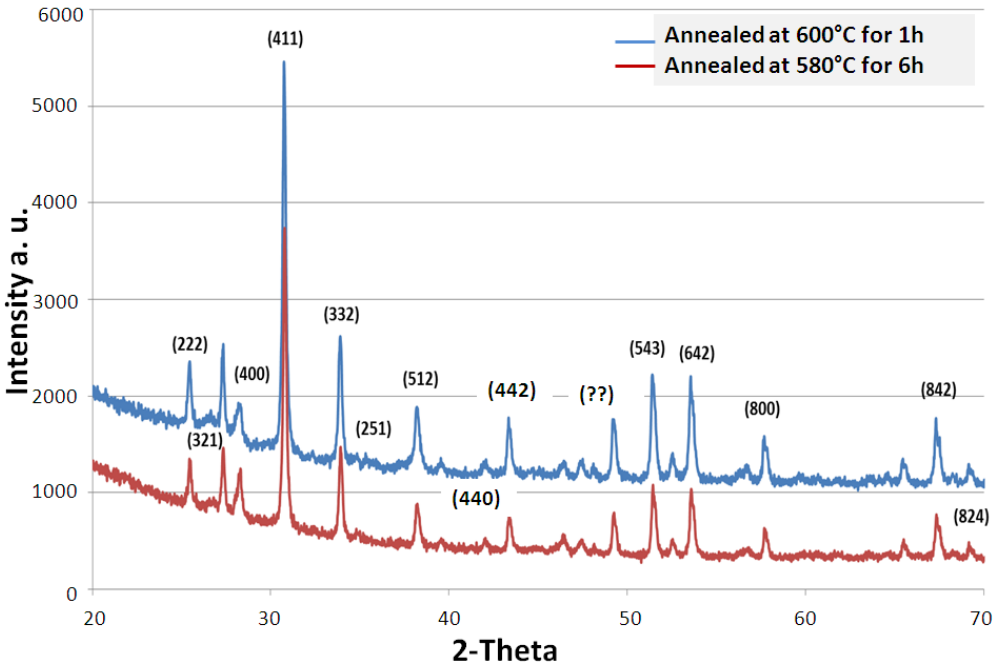

Fig. 1. X-ray diffraction data sets obtained from two garnet layers deposited onto glass substrates from a sputtering target of composition type $Bi_{2.1}Dy_{0.9}Fe_{3.9}Ga_{1.1}O_{12}$. The garnet films were optimally annealed.

It is important to note that, as in many other cases of new garnet compositions development, the observed peaks near 45-46 degrees correspond to Fe_3O_4, however, using the search function to predict other oxides, such as Fe_2O_3, Bi_2O_3, Ga_2O_3 and Dy_2O_3, ambiguous results were obtained, revealing the presence of many combinations of oxides. The average calculated (using the data from several indexed peaks) lattice constant of the film layer material, formed as a result of crystallizing the layers originating from sputtering the target of $Bi_{2.1}Dy_{0.9}Fe_{3.9}Ga_{1.1}O_{12}$ on the substrate, was found to be 12.515 Å while the expected cubic lattice parameter of this garnet composition was about 12.521 Å [22]. According to this calculation it seems that possibly a garnet layer containing Bi substitution level of up to 2 formula units (f. u.) was synthesized. From the XRD data of the annealed garnet samples, the crystallite size of the garnet films was calculated using Scherrer equation, namely, $Dp = K\lambda / \beta\cos\theta$ [22,24,25] where the value for the shape factor K is 0.94 and the X-ray wavelength $\lambda = 0.154056$ nm were used. The measured average crystallite size for this garnet layer was about 37 nm.

Optical Materials EXPRESS

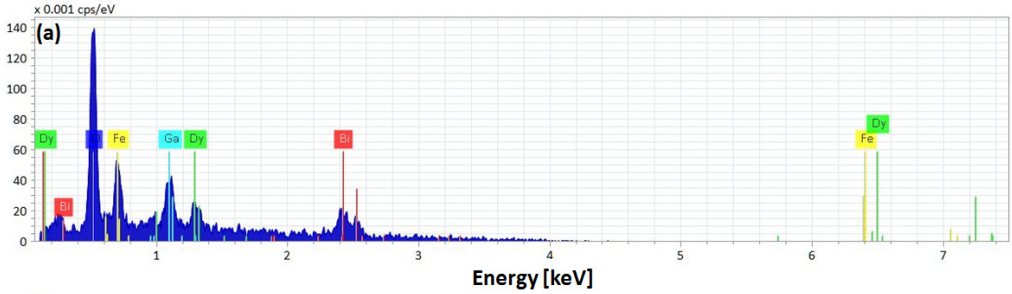

(b)

Element	At. No.	Netto	Mass [%]	Mass Norm. [%]	Atom [%]	abs. error [%] (1 sigma)
Oxygen	8	116	12.86	27.88	66.12	6.08
Iron	26	58	13.05	28.28	19.21	8.16
Dysprosium	66	10	2.81	6.08	1.42	1.01
Gallium	31	35	8.14	17.63	9.60	1.70
Bismuth	83	10	9.29	20.12	3.65	3.20
		Sum	**46.14**	**100.00**	**100.00**	

(c)

Element	At. No.	Netto	Mass [%]	Mass Norm. [%]	Atom [%]	abs. error [%] (1 sigma)
Oxygen	8	125	8.52	27.32	68.81	3.93
Bismuth	83	12	8.17	26.18	5.05	2.61
Iron	26	53	7.24	23.22	16.75	4.74
Dysprosium	66	21	3.84	12.30	3.05	0.99
Gallium	31	23	3.42	10.97	6.34	0.87
		Sum	**31.19**	**100.00**	**100.00**	

Fig. 2. EDS microanalysis results obtained from optimally annealed garnet thin films of composition type $Bi_{2.1}Dy_{0.9}Fe_{3.9}Ga_{1.1}O_{12}$. (a) Typical measured EDS spectrum of a 1 micron-thick garnet sample prepared on glass substrate; (b) and (c) EDX composition measurement data obtained from a 200 nm (b) and a 1000 nm (c) thick garnet samples, respectively. These elemental measurements were performed using multiple scans in different spots on the sample, and the best average data were considered for sample analysis.

EDS microanalysis experiments were carried out to determine the elemental composition of the thin garnet films. For each sample the EDS measurements were performed several times (at least five) on different spots on the sample surface, to obtain the most consistent and accurate compositional information. The measured elemental concentrations (in atomic %) confirmed the presence of all elements expected to be present within the films, as shown in Fig. 2. Based on these measurement data, the derived composition of the garnet thin films prepared on glass substrates was $Bi_{(2 \pm 0.13)}Dy_{(1 \pm 0.13)}Fe_{(3.48 \pm 0.15)}Ga_{(1.52 \pm 0.15)}O_{12}$. This composition was expected to be attained considering the sputtering target's nominal stoichiometry ($Bi_{2.1}Dy_{0.9}Fe_{3.9}Ga_{1.1}O_{12}$) and the sputtering conditions. The ratio between the Fe and Ga content and oxygen content in terms of atom number per formula unit was found to differ slightly from the expected ratio, and this is attributed to the experimental errors related to the detection of the reflection spectrum from the sample's surface, generated by the X-rays incident on the sample.

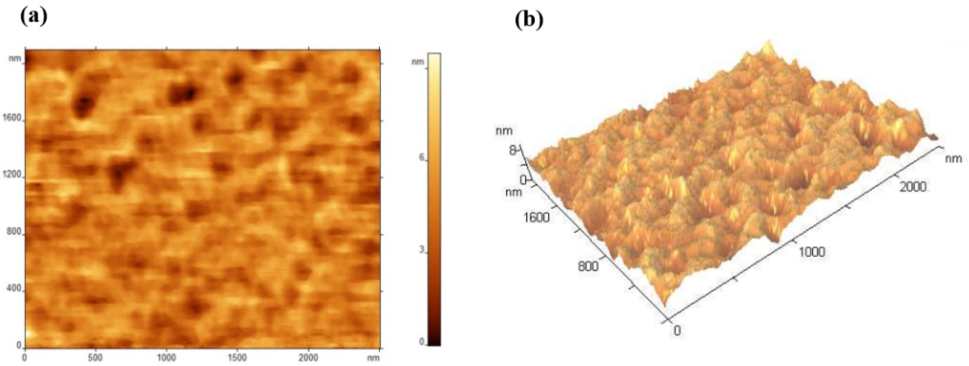

Fig. 3. AFM images of an annealed garnet layer prepared on a Si substrate. (a) 2D surface morphology and roughness scale. (b) 3D image of the same area of size 2.5 µm x 2 µm. The garnet layer was annealed at 620°C for 3h.

Optical Materials EXPRESS

The surface morphology of a garnet film prepared on a silicon (Si) substrate was investigated by using an atomic force microscope (AFM) and the results are shown in Fig. 3. The thickness of the investigated garnet layer was about 250 nm. The values of the measured average roughness (R_a), mean-square roughness (R_q) and the roughness height (R_z), measured at 10 points, were around 1.457 nm, 2.103 nm, and 4.903 nm, respectively.

Note that the surface quality of films grown on glass substrates practically always exceeded the quality of films grown on silicon. The AFM images shown in Fig. 3 are particularly important because they reveal that small-size grains and relatively flat surface morphologies are also achievable on silicon substrates, using similar annealing regimes.

Figure 4 shows the derived absorption coefficients spectra of garnet thin film layers (prepared using optimized fabrication process and later annealed at different temperatures and process durations). Very similar trends of absorption coefficients spectra were observed across the visible spectral region, despite slight variations for films annealed at higher temperatures. However, those films possessed high Faraday rotations, and hence high MO figures of merit. The low-absorption performance achieved in the optimally annealed garnet films of this composition type (measured absorption coefficients at 532 nm were in-between 5000 and 6000 cm^{-1}) is very comparable with that of epitaxially deposited monocrystalline films. The magnetic behaviour of the garnet thin films grown on glass substrates was investigated based on the obtained values of specific Faraday rotation and MO figure of merit. Fitting the measured and modeled transmission spectra (Fig. 4) of the garnet films enabled the actual garnet layer thickness to be measured and also the optical absorption coefficient (α cm^{-1}) of the optimally annealed garnet thin films derived [15,20]. The values of specific Faraday rotation and MO figures of merit of the annealed garnet films were calculated using the following formulas:

$$Specific\ Faraday\ rotation \Theta_F = Rotation\ angle\ (one\ way) / Film\ thickness\ (^\circ / \mu m) \quad (1)$$

$$MO\ figure\ of\ merit\ Q = 2 * \Theta_F / a\ (deg) \quad (2)$$

where α is optical absorption coefficient.

The MO figures of merit for all (annealed) samples were calculated taking into account the measurement errors in the films' thickness (within estimated ± 5% accuracy) as well as in Faraday rotation angles (measured with a maximum error of ± 0.05°). The setup for measuring the specific Faraday rotation is described in Ref [19].

Optical Materials EXPRESS

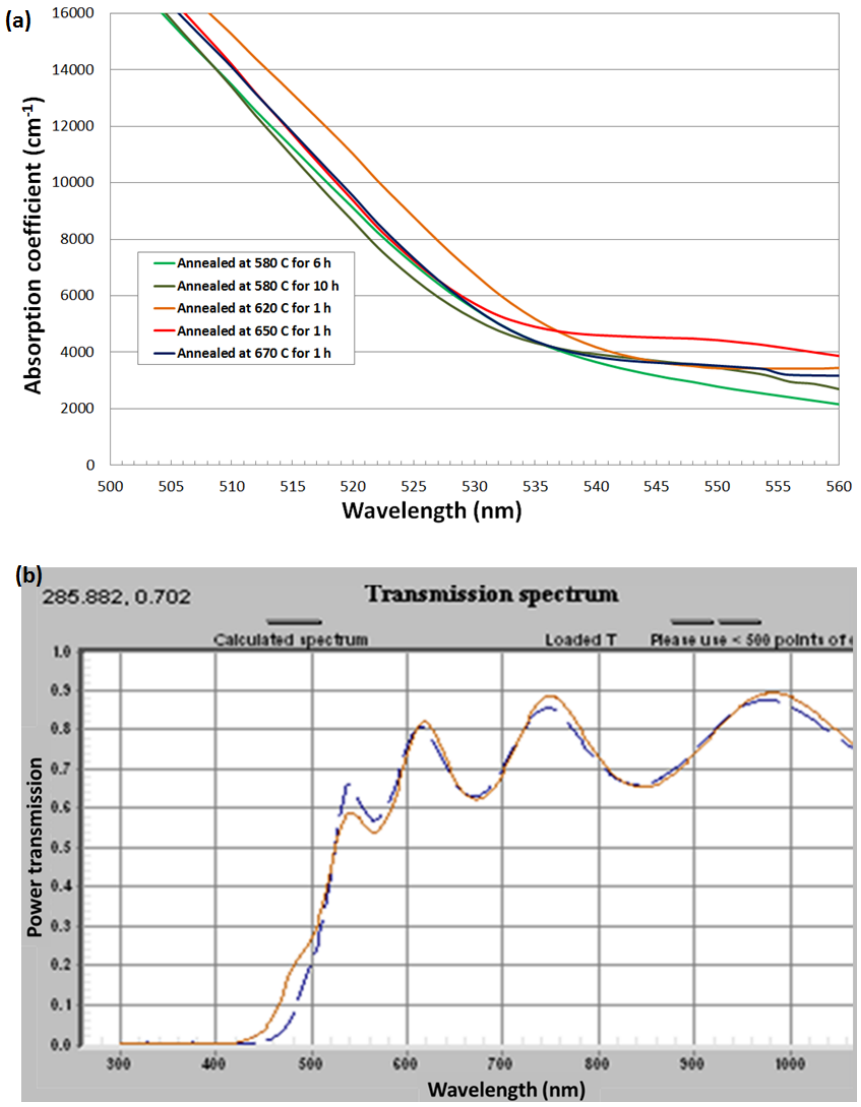

Fig. 4. (a) Derived absorption spectra of the garnet layers annealed at different annealing temperatures and process durations. The annealing regimes used to crystallize the garnet layers are mentioned. (b) Illustration of the peak-by-peak fitting of the measured (light orange continuous line) and modeled (blue dotted line) transmission spectra of a garnet layer. The refractive index spectra of garnet films obtained from wide-angle spectroscopic ellipsometry measurements were also used in software-assisted absorption coefficient fitting.

The garnet layer thickness was first measured directly during film deposition, using a well calibrated quartz sensor. Using the measured transmission spectrum and refractive index data, it is typically possible to re-confirm the actual thickness of the garnet layer through very close fitting of the measured and simulated transmission spectra. In experiments that also involved SEM imaging of the film cross-sections, all three measured (or fitted) thickness values were typically within ± 5nm accuracy. Once the thickness has been fitted, in-house-developed software was used to fit the absorption coefficient spectrum using the thickness values, fitted transmission spectrum, and the known n and k spectra of the garnet material.

Optical Materials EXPRESS

Note that, while the absorption coefficient is comparable to absorption coefficients attained using other possible deposition processes, our sputtering process is particularly scalable, hence enabling the mass production of garnet-based devices cost-effectively.

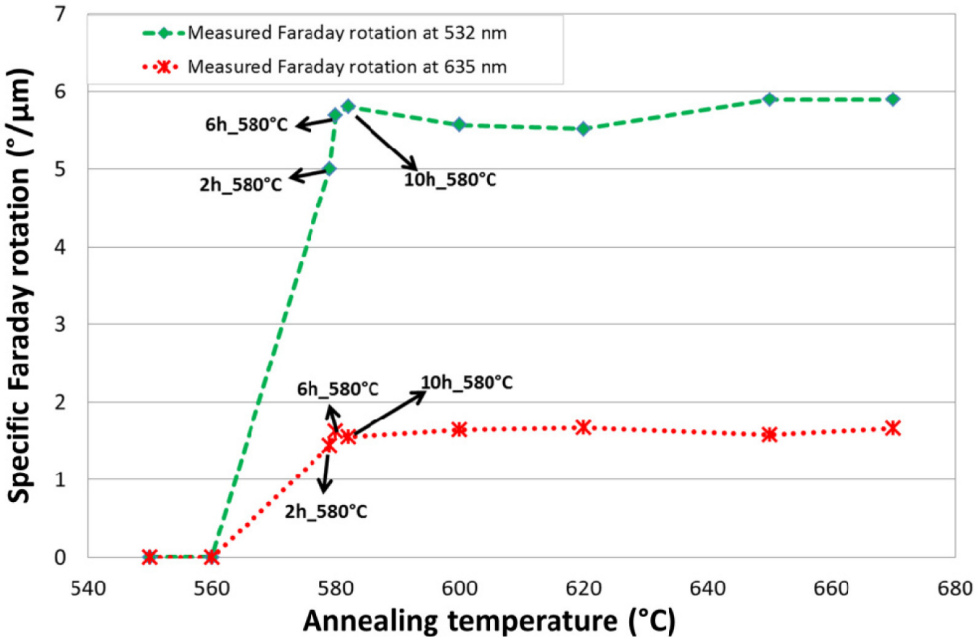

Fig. 5. Measured specific Faraday rotation data points for 532 nm and 635 nm light for garnet layers sputtered onto glass substrates and subjected to different annealing regimes (temperatures and process durations are shown).

Figure 5 shows the measured specific Faraday rotation of the garnet layers for 532 nm (green dotted line) and 635 nm (red dotted line) light, as a function of the annealing temperatures. It can be noted that at 532 nm, a drop in the specific Faraday rotation with increasing annealing temperature was observed after 580°C (the best performance at 580 °C was seen after running a 10h-long process). After the annealing temperature reached 650°C, an improvement in specific Faraday rotation was again observed. The measured MO figures of merit data points for the optimally annealed garnet films are plotted against their annealing regimes (Fig. 6). The best MO figures of merit achieved were 24.4° at 532 nm (in samples annealed at 580°C for 10h) and 19.8° at 635 nm (in samples annealed at 580°C for 6h). For process temperatures higher than 580°C, the Faraday rotation values increased, however, some film surface degradation was observed, which increased the scattering losses, and consequently, reduced the achievable MO figures of merit at 635 nm. These observations were generally consistent with the effects of annealing process parameters on film quality observed by our group previously in various thin-film garnet composition types [15,20].

Optical Materials EXPRESS

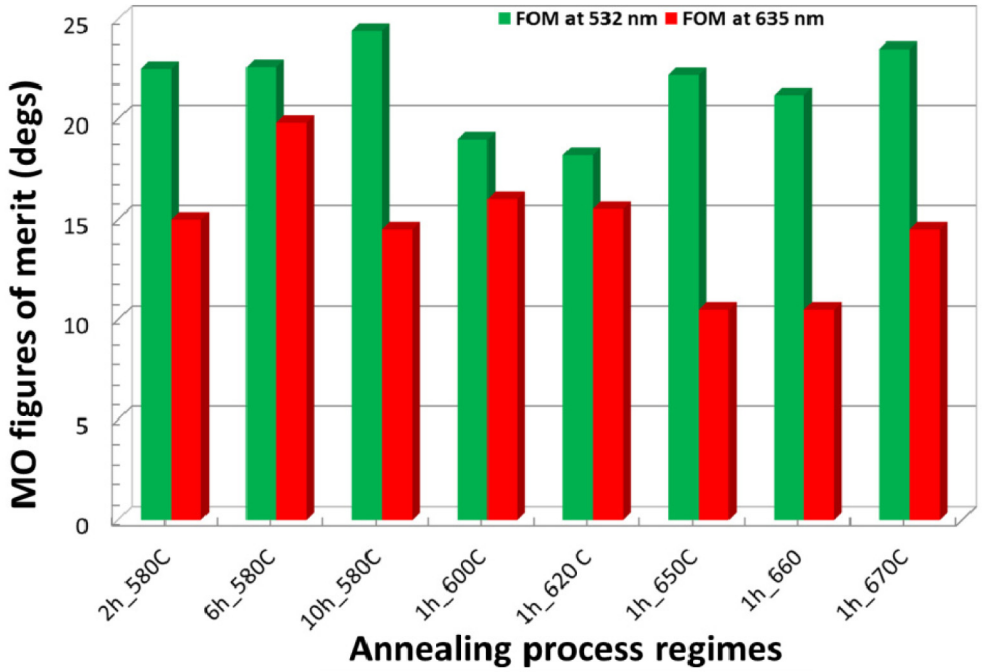

Fig. 6. Values of MO figure of merit at 532 and 635 nm obtained in annealed garnet films, presented against the annealing regimes (temperatures and process durations) used to anneal the garnet layers after the sputtering deposition process.

The MO figures of merit reported within this article may not be world-record high (that is difficult to prove due to a general lack of published data on this parameter and a large number of garnet compositions possible), yet, the actual garnet composition is entirely new and has never been reported to be synthesized using sputtering processes. The reported MO figure of merit near 25 degrees at 532 nm is relatively high, which is attributed to the superiority of the composition of the developed garnet material, in comparison with garnet compositions reported to possess record-high MO quality (Ref. 15). Note that the difference between the MO responses at 532 nm and 635 nm generally originates because of the UV absorption tail associated with the magneto-optic transition, leading to strong MO Faraday rotation near the blue spectral region. Note also that the exponential decay of MO Faraday rotation with wavelength is typical of MO garnet materials.

Magnetic hysteresis loops of specific Faraday rotation of two annealed garnet films measured at room temperature are shown in Fig. 7. Very similar shapes of the hysteresis loops were obtained with the minimum coercive field of about 30 Oe; and the saturation magnetization values were less than 500 Oe for both films. The linearity of these hysteresis curves of specific Faraday rotation indicates that the films possess an almost in-plane magnetization vector direction. This is attractive for the development of nano-engineered artificial magnetic media, e.g., magneto-plasmonic crystals as well as other emerging and existing nanophotonics micro-devices, including magnetic field sensors and visualizers.

Optical Materials EXPRESS

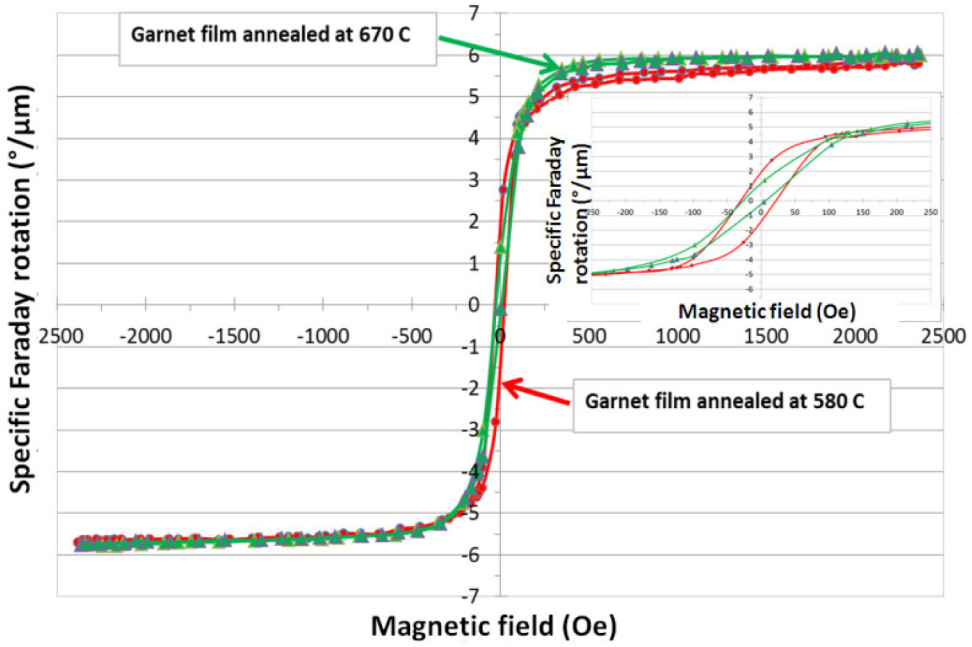

Fig. 7. Measured hysteresis loops of Faraday rotation as a function of applied magnetic field for two annealed garnet samples. Inset shows the achieved low coercive field and saturation magnetization values.

The high MO figures of merit, low coercive field and relatively high Faraday rotation angles achieved in sputtered films of this garnet material make them particularly suitable for use in specialized nanophotonics applications which require a specific combination of the optical, magnetic, and magneto-optical properties demonstrated in films of this composition. A notable feature of sputtered $Bi_{2.1}Dy_{0.9}Fe_{3.9}Ga_{1.1}O_{12}$ layers on glass substrates include their "intermediate" magnetic anisotropy type, featuring an almost in-plane magnetization and a very "narrow" hysteresis loop concurrently with magnetic memory properties (with the Faraday rotation at remnant magnetization being near 25% of its saturated value). This makes it possible to use these films in magnetic field visualizers that can generate either permanent images of magnetic field distributions (using perpendicular or out-of-plane imaging regime reliant on magnetic memory of films), or the in-plane (analogue) images. To the best of our knowledge, no published literature sources have reported so far on the synthesis and characterization of garnet thin films of this particular stoichiometry type or possessing a combination of properties reported here, at least within the field of RF sputtering deposition.

5. Conclusion

We have prepared films of a highly Bi-substituted iron garnet material of composition $Bi_{2.1}Dy_{0.9}Fe_{3.9}Ga_{1.1}O_{12}$ using RF magnetron sputtering in pure argon (Ar) plasma. The garnet films have been optimally annealed to attain high Faraday rotation and low optical absorption over a wide spectral range. Experimental results have shown that the developed garnet films exhibit high MO performance, low coercive force of around 30 Oe and almost in-plane magnetic properties. This type of Bi-substituted iron garnet materials is attractive for the development of magneto-optical sensors, magnetically switchable transparency elements and integrated optical isolators.

Funding

Electron Science Research Institute, Edith Cowan University, Australia.

139.230.245.23 {ts '2017-03-04 02:21:05'}